# 11

# Commercial Exploitation of Zooplankton in the Norwegian Sea

Eduardo Grimaldo and Svein Helge Gjøsund
*SINTEF Fisheries and Aquaculture*
*Norway*

## 1. Introduction

Since 1990s there has been increased interest in the exploitation of marine zooplankton like copepods and krill. This has been motivated by the increasing demand for marine bio-resources for human consumption in general, and in particular the growing demand for feed in aquaculture. In Nordic Seas, zooplankton is a key component in the energy transfer from primary producers to higher trophic levels such as herring, capelin, salmon, cod larvae and juveniles, and other species (Skjoldal, 2005). Roughly 70-80% of the zooplankton production in these waters is made up by copepods of the genus *Calanus* (Tande and Miller, 2000). According to general ecological theory about 10% of this production is available to the next trophic level (Lalli and Parsons, 1997). Estimates of the total annual production of *Calanus sp*. vary between 75 million tons $y^{-1}$ for the Nordic Seas (Aksnes and Blindheim 1996) and 300 million tons *Calanus sp*. (mainly C*alanus finmarchicus*) $y^{-1}$ for the Norwegian Sea only (Skjoldal et al. 2004).

This vast resource has great economic potential because it is rich in marine lipids, proteins, amino acids, and pigments. Further, by nature of being low on the food chain it has far lower bioaccumulation of heavy metals, organo-chlorides, dioxins, and other pollutants than higher trophic species now in use (Mizukawaa et al., 2009). Therefore, copepod fisheries have a potential to support the growth of new ventures in markets for functional food, food ingredients, and nutrition products. However, development of a copepod fishery must be pursued wisely (Nicol and Endo, 1999) using the best technology at hand, and implemented within a solid ecosystem based management regime, particularly given the importance of copepods to the marine ecosystem. In open Norwegian waters, *Calanus finmarchicus* is widely found in the upper 50 m during the productive period from April to August (Falkenhaug et al., 1997; Dahle and Kaartvedt, 2000). For practical reasons, harvesting concentrates on adults (CVI) and the life stages CIV and CV (the two last copepodite stages before becoming adults), because in these stages copepods have achieved sufficient body mass - body lengths are from 2.3 to 5.0 mm - depending upon species (Unstad and Tande, 1991). In addition, lipid content of copepods increases with increasing stage, with the two oldest stages being the most lipid rich (Kattner and Krause 1987).

Currently, *Calanus finmarchicus* harvesting uses fine-meshed trawls (~500 µm bar length) with mouth openings that range from 40 to 100 $m^2$, depending on the vessel size (Snorre Angell, Calanus AS, Sortland-Norway, Pers. Comm., 2009). However these trawls may be

unsuitable for large-scale zooplankton harvesting because their very high towing resistance translates to high fuel consumption and $CO_2$ emissions.

## 2. Zooplankton trawls

In Norway, the development of commercial harvesting of zooplankton (*Calanus finmarchicus*) started in the fjords in the late 1950's, with relatively small nets operated from smaller boats (Wiborg and Hansen, 1974). The fishery developed from annual catches of a few tons to more than 50 metric tons by the mid 1970's. By then one had also developed larger trawl-like structures, e.g. beam trawls with rectangular front openings up to 5 m wide and 4 m high, and with coarser jellyfish nets at the front and structural cover nets outside the filtering net (Wiborg and Hansen, 1974). The fishery then evolved only slowly, but through the 1990's there was an increasing interest for *Calanus finmarchicus* as a potential raw material for feed in the rapidly growing aquaculture industry. For precautionary reasons, a general prohibition against harvesting of zooplankton in Norwegian waters was introduced in 2006. In order to support the further development of a sustainable fishery the authorities instead granted a limited annual trial quota for *Calanus finmarchicus.* The trial fishery has been conducted by the Norwegian biomarine company Calanus AS, who developed and patented a harvesting system for *Calanus finmarchicus.* Their trawls have ~ 500 µm meshes and front areas of up to 100 $m^2$ (~12 m wide, ~8 m high), with reported catch rates up to 2 tons dried weight per hour (Snorre Angell, Calanus AS, pers. comm.) (Fig 1).

Fig. 1. Full scale test of a commercial zooplankton trawl (left), and 1200 kg of copepods (*Calanus* sp.) caught after one hour tow (right). Photo: Snore Angell, Calanus AS.

By 2011 the Norwegian Ministry of Fishery and Coastal Affairs are preparing a public hearing to prepare for a limited, but more open commercial fishery for *Calanus finmarchicus.* In addition, the company Plantonic AS has being granted a special permit to harvest also smaller phyto- and microzooplankton, e.g. as an alternative to cultivated feed for the larval and juvenile stages of cultured fish species. For the latter large, anchored (stationary) nets are used. Mesh sizes can be an order of magnitude or smaller than those used for adult *Calanus finmarchicus*, posing considerably greater challenges with respect to filtration and clogging.

### 2.1 Flow through plankton nets and trawls

A theoretical model for the flow through fine-meshed nets and trawls is presented in Gjøsund and Enerhaug (2010). They derive basic relations for the flow through and forces on inclined net sections, based on pressure drop and streamline deflection through porous screens, and present parametric expressions for the filtration efficiency and drag on conical nets, cf. Eqs. 1 and 2. The model allows easy assessment of the effect of varying mesh opening, twine thickness, porosity, taper angle and flow (towing) velocity. The filtration efficiency F is defined as the ratio between the average velocity across the net mouth and the velocity of the net through the water (e.g. the towing velocity through quiescent water), see Figure 2. Further in Eqs. 1 and 2, $C_D$ is the overall drag coefficient, $F_D$ is the overall drag force, $A_0$ is the mouth area, $C_N$ is a normal force coefficient, K is the pressure drop coefficient, $K_0$ is K($a$ = 90°), $Re_d$ is the effective Reynolds number, d is twine diameter, $\nu$ is kinematic viscosity, $a$ is taper angle, $\gamma$ is an angle describing streamline deflection, $\beta$ is the screen porosity, $T_\gamma$ is a tangential stress coefficient due to streamline deflection, and $T_f$ is a tangential stress coefficient due to friction. The expression for $K_0$ in Eq. 4 is from Brundrett (1993), $C_N$ in Eq. 6 is from Løland (1991), $\gamma$ in Eq. 7 is from Gibbings (1973) and the tangential stress component in Eq. 8 is from Taylor and Batchelor (1949). Schubauer et al. (1950) found that Eq. 5 describes the pressure drop well for $a \geq 45°$, and Gjøsund and Enerhaug (2010) argue that it applies to lower taper angles also if the Reynolds number dependency in $K_0$ is properly accounted for. A suitable model for $T_f$ is not available, and Gjøsund and Enerhaug use a constant value $T_f$ = 0.02. A number of other models for $K_0$ and $C_N$ exist, see Gjøsund (2006) and Gjøsund and Enerhaug (2010), and may yield equally good or better predictions is some cases. Gjøsund and Enerhaug (2010) conclude that the filtration efficiency is well predicted by Eq. 1 invoking Eqs. 3-6, while there is more uncertainty related to $C_D$ in Eq. 2, presumably due to Eq. 7 being less accurate at smaller taper angles. Note that Eq. 1 is a simplification of the corresponding expression in Gjøsund and Enerhaug (2010, their Eq. 16), and that it must be solved in an iterative manner because K is also a function of F.

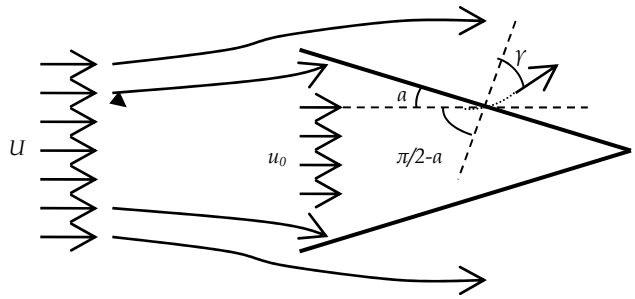


Fig. 2. Sketch of flow through a conical net with taper angle α and filtration efficiency F = $u_0$/U, the angle γ describes streamline deflection through the net wall ("cf." from Gjøsund and Enerhaug, 2010).

$$F = \frac{u_0}{U} = \sqrt{\frac{C_N(K)}{K}} \tag{1}$$

$$C_D = \frac{F_D}{1/2\rho U^2 A_0} = C_N(K) + \frac{F^2\left(T_\gamma + T_f \sin^2(\alpha+\gamma)\cos^2\left(\frac{\pi}{2}-\gamma\right)\right)}{\tan\alpha} \tag{2}$$

$$Re_d = \frac{(u_0 \sin\alpha)d}{\upsilon} \tag{3}$$

$$K_0 = \left[\frac{7.0}{Re_d} + \frac{0.9}{\log(Re_d + 1.25)}\right]\frac{1-\beta^2}{\beta^2}, 10^{-4} < Re_d < 10^4 \tag{4}$$

$$K = K_0 \sin^2\alpha \tag{5}$$

$$C_N(K) = \frac{2}{K}\left[K + 1 - \sqrt{2K+1}\right] \tag{6}$$

$$\gamma = \tan^{-1}\left[\Delta \tan\left(\frac{\pi}{2} - \alpha\right)\right], \Delta = \left[\left(\frac{K_0}{4}\right)^2 + 1\right]^{\frac{1}{2}} - \frac{K_0}{4}, 0 < \gamma < \frac{\pi}{2} - \alpha \tag{7}$$

$$T_\gamma = \frac{\tau}{1/2\rho u_0^2} = 2\sin^2\alpha\left[\tan\left(\frac{\pi}{2} - \alpha\right) - \tan\gamma\right], 0 < \gamma < \frac{\pi}{2} - \alpha \tag{8}$$

A key element in Gjøsund and Enerhaug (2010) is the importance of viscous effects at very low Reynolds numbers, i.e. as local dimensions and velocities become very small. This Reynolds number effect manifests itself as a dramatic increase in the pressure drop coefficient as mesh dimensions and towing velocities decrease; potentially leading to a strong decrease in filtration efficiency, see Eq. 1 and Figure 2. Hence the filtration efficiency of plankton nets depends strongly on the net parameters and towing velocity. Gjøsund and Enerhaug (2010) compare the theoretical model with flume tank measurements with fine-meshed net cones, and demonstrate among other things how the filtration efficiency for typical plankton nets increases with increasing towing velocity, and decreases with decreasing velocity (Figure 3). This is contrary to common belief, as noted also by Tranter and Heron (1967); there is a widespread and persistent, but incorrect perception that filtration efficiency generally decreases as towing velocity increases. In plankton sampling the towing velocity is therefore often recommended to be low, and it is also assumed that a low towing velocity reduces clogging (Sournia, 1978). However, Tranter and Heron (1967) found that so-called flared samplers clogged more readily in field experiments than unflared samplers. A flared sampler implies reduced velocity inside the net and towards and through the net wall, hence hydrodynamically it is equivalent to an unflared sampler with lower filtration efficiency. Also, as the velocity decreases and the pressure drop coefficient increases, the flow (and thus the plankton) deflects more perpendicularly towards the net wall (Reynolds, 1969), i.e. the angle $\gamma$ in Figure 3 decreases. This suggests that the clogging rate may actually increase with decreasing velocity in some cases. Here it is crucial to consider clogging with respect to filtered volume and not with respect to tow time or tow distance (McQueen and Yan, 1993); if one measures reduced clogging at low velocities compared to higher velocities, this may simply be due to the low velocity case filtering less water and thus less plankton than assumed. For high towing velocities, e.g. 10 knots and more as sometimes used in so-called high speed sampling, other effects may be important and it is less clear how velocity variations affect filtration. For instance, the global wake field behind the sampler can influence filtration to a greater extent.

Usually only the open area ratio R is considered when designing plankton nets, i.e. the ratio between the open mesh area and the mouth area. A general recommendation is that R should be greater than 3 to have high initial (i.e. before any clogging occurs) filtration

efficiency (Tranter and Heron, 1967), and greater than 6 to have an additional buffer against clogging (Harris et al., 2000). However, this ratio involves only the porosity and taper angle of the net; it does not account for the Reynolds number effect described above. Figure 3 shows that recommending low towing velocities and a fixed value of R can be highly misleading in some cases, and may result in low filtration efficiency and potentially also in increasing clogging. This may represent a significant and largely unknown source of error in plankton samples and abundance estimates, in particular for the very smallest plankton and mesh sizes. There are nevertheless other reasons for limiting the towing velocity. If the pressure becomes too high, very fine meshed netting may break (Sournia, 1978), and plankton may be extruded through the meshes and thereby lost or contributing to clogging. Also, the towing resistance basically increases with the towing velocity squared. This is seldom an issue for small sampling nets, but it can be crucial for the fuel efficiency of larger commercial plankton trawls. For commercial plankton trawls, key issues are catch quality, catch- and fuel efficiency and structural reliability, requiring that filtration efficiency, clogging, towing resistance and more are properly balanced in the design process (Larsen, 2009).

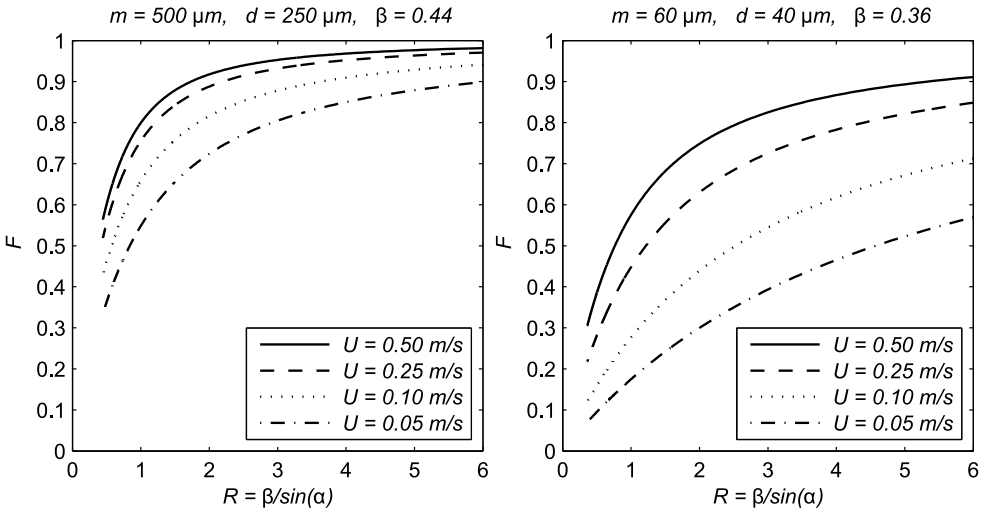


Fig. 3. Predicted initial filtration efficiency F as a function of open area ratio R for two nets with different mesh size m, twine thickness d and porosity β, at four different velocities 5, 10, 25 and 50 cm/s (from Eq. 1, cf. Gjøsund and Enerhaug, 2010).

## 3. Bubble-enhanced zooplankton harvesting

Bubble-enhanced zooplankton harvesting is a novel environmental friendly platform for commercial harvest of zooplankton at sea, targeting lower energy consumption during towing and less by-catch than existing catching equipment. The working principle of this harvesting platform is based on releasing air bubbles at a depth of 20-40 meter to vertically displace copepods towards the sea surface. Key components are a submerged, towed air bubble diffuser (sparging elements), an air delivery system, and a collector net or surface skimmer (Fig 4).

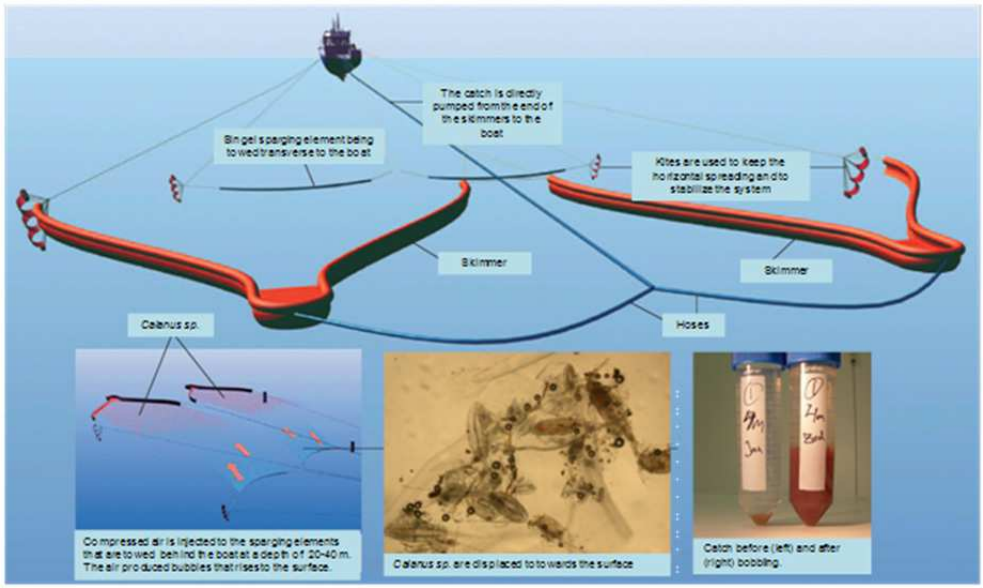


Fig. 4. Initial prototype of a skimmer trawl for commercial harvesting of *Calanus sp*. Air is released from a single perforated hose at 20-40 m depth to produce small bubbles. These bubbles while rising displace *Calanus sp* towards the surface. Here they are collected by skimmer and directly pumped to the boat. Animation: Mats Heide, SINTEF.

Two primary mechanisms associated with micro-bubble technology are upwelling (Leifer et al., 2009) and attachment/flotation. As bubbles rise, they transfer momentum to the surrounding fluid, creating the upwelling flow, which transports deeper water upwards, including entrained zooplankton. For bubble attachment, small bubbles attach and add positive buoyancy to the zooplankton, lifting them upwards. Real-world applications involve both of these synergistic processes.

### 3.1 Bubble attachment

Bubbles effectively accumulate surfactants through the process termed sparging or flotation. Surfactants are surface active substances including surfactant-bacteria and particles with hydrophilic and hydrophobic sites that energetically prefer to be at air-water interfaces. This bubble collection and transport process is central to wastewater treatment microflotation (Persechini et al., 2000), mining airlift separators (Mao and Yoon, 1997), bioreactors (Wu, 1995), and marine aggregate formation (Mari, 1999). Surfactants affect bubble properties, decreasing gas exchange and rise velocity and thus decreasing dissolution (Leifer and Patro, 2002). Surfactants also stabilize bubbles against breakup (Johnson and Cooke, 1980). Attachment requires several steps. First, the bubble trajectory must intersect the zooplankton close enough for the two to touch. Then, the bubble and zooplankton must attach, rather than "bounce." Finally, the bubble must remain attached long enough to lead to significant vertical advection. Smaller (< 300 μm radius) bubbles are more likely to attach to *Calanus* because of their slower rise velocities (< 6 cm $s^{-1}$), and because their size is

comparable to key *Calanus* dimensions, such as thorax, legs, and antennae. However, because small bubble buoyancy is minimal, they provide little lift buoyancy force. Given that *Calanus* are slightly negatively buoyant; this can lead to minimal or negligible upwards motion unless several small bubbles attach to the copepod.

Laboratory studies showed that the highest zooplankton attachment was for bubbles in the range $50 < r < 300$ µm (own data, unpublished), where $r$ is the equivalent spherical radius (Fig. 5). Although larger bubbles have greater buoyancy, their attachment probability is lower (own data, unpublished). Bubbles comparable in size or larger than *Calanus* - circa 1000-µm radius - have well developed turbulent wakes and boundary layers, and rise fast (25 – 30 cm $s^{-1}$) compared to small bubbles (Leifer and Patro, 2002). These large bubbles tend to displace the *Calanus* along streamlines around the bubble as they pass, leading to negligible attachment probability. After attachment, the bubble-copepod aggregate rises with a velocity, $V_{AG}$, determined by the drag resistance of the *Calanus*-bubble aggregate and the buoyancy force, until bubble detachment (or surfacing). In laboratory studies, a linear relationship was found between $r$ and $V_{AG}$, from 2.5 to 9.0 cm $s^{-1}$ with the highest rise velocity for a 341-µm radius bubble (own data, unpublished). Because *Calanus* are mobile, bubble detachment by body motions can be significant and reduces the *Calanus* vertical advection distance. Then, a combination of *Calanus*'s negative buoyancy and active swimming towards its original depth likely will cause sinking. Thus, successful flotation requires the attachment time scale to be sufficiently shorter than the detachment time scale. Due to detachment, flotation of more active *Calanus* is less efficient, mimicking natural selection.

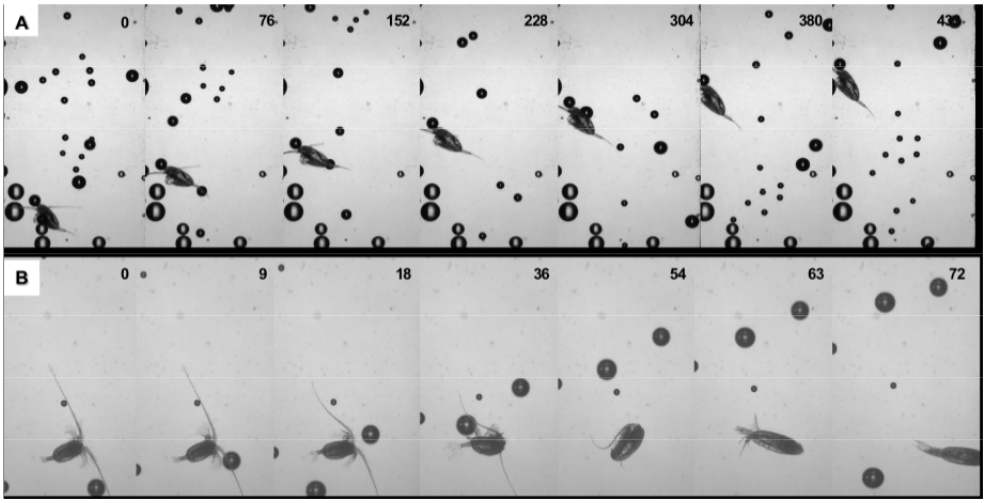


Fig. 5. *Calanus* response to bubbles (timestamp in images is given in milliseconds). A) One $r$~150-µm bubble attaches to a *Calanus* head, causing upwards motion. B) Detachment of a small bubble ($r$~75 µm) from the *Calanus* antenna during an escape jump, possibly triggered by a passing larger bubble ($r$~350 µm).

### 3.2 Bubble-driven upwelling flow

For sufficiently high bubble concentration, synergistic interactions in bubble plumes create fluids with distinct properties from the surrounding fluid (Leifer et al., 2006). Bubble plumes transfer momentum to the surrounding fluid; creating an upwelling flow, see review in Leifer et al. (2009). The upwelling flow decreases bubble gas exchange with the surrounding fluid because of the reduced transit time across the water column, enhancing bubble survival against dissolution (Leifer et al., 2006).

For point-source bubble plumes, larger fluid velocities are at a peak along the centerline decreasing radially with a Gaussian profile (Milgram, 1983). The fluid velocity increases with height above the source in non-stratified fluids due in part to the increase in buoyancy flux from decreasing hydrostatic pressure. At the surface, the upwelled fluid spreads out in a horizontal intrusion, the outwelling flow. Thermal and haline stratification are common in the marine environment, with cooler and/or more saline (denser) water at greater depth. Thus, marine upwelling flows lift water with increasingly negative buoyancy. Upon encountering a steep density gradient, the bubble plume can significantly (or completely) detrain plume fluid into a horizontal intrusion; however, the bubbles continue rising, entraining new water, unlike for a continuum (single phase) plume such as a sewage outfall (McDougall, 1978). Such horizontal intrusions deposit any transported zooplankton, marine particles, and dissolved gases in a layer, and have been identified in the field (Solomon et al., 2009; Leifer et al., 2009; Leifer and Judd, 2002). Sufficiently strong bubble plumes can support the upwelled fluid through the density stratification to the sea surface.

Laboratory studies showed that upwelling advection has "100%" efficiency (the analogue of bubble attachment) for copepods entrained in the flow, and created faster vertical motions than flotation (own data, unpublished). Moreover, where the upwelling flow is wide copepod jumps cannot exit the upwelling flow (analogue of detachment). Bubble plumes were produced for flow rates, $Q$, spanning $0.48 < Q < 76.5$ L h$^{-1}$ which produced upwelling flows, $V_{up}$, from $4 < V_{up} < 37$ cm s$^{-1}$, with the highest $V_{up}$ for flows with large bubbles or large Qs. For this study, $V_{up}(Q)$, showed a power law increase with $Q$ as $V_{up}(Q) \sim Q^{0.20}$ for small bubbles ($r$ ~ 50-100 μm) and $V_{up}(Q) \sim Q^{0.33}$ for large bubbles ($r$ ~ 400-600 μm), in close agreement with the large-scale plume findings of Leifer et al. (2009), who found $V_{up}(Q) \sim Q^{0.23}$, and also for seep bubble plumes in the open ocean (Leifer, 2009) where $V_{up}(Q) \sim Q^{0.3}$. These parameterizations are in agreement with the finding of the calculations of Lemckert and Imberger (1993) on the Milgram (1983) data set.

### 3.3 Stationary vs towed bubble plumes

Most published field bubble plume studies are for stationary bubble plumes in static water (e.g., lake destratification studies) (Schadlow, 1992; Lemckert and Imberger, 1993; Singleton et al., 2007), natural marine hydrocarbon seeps (Leifer et al., 2000; Leifer and Boles, 2005; Leifer et al., 2009), or gas blowouts (Topham, 1975; Milgram, 1983). However, typical fisheries applications involve a towed bubble plume (Grimaldo et al., 2010). Potentially, there is a significant difference between a stationary (i.e., fixed) source bubble plume in a uniform horizontal current (Fig. 6A) and a towed source bubble plume through quiescent water (Fig. 6B), even though both geometries appear similar.

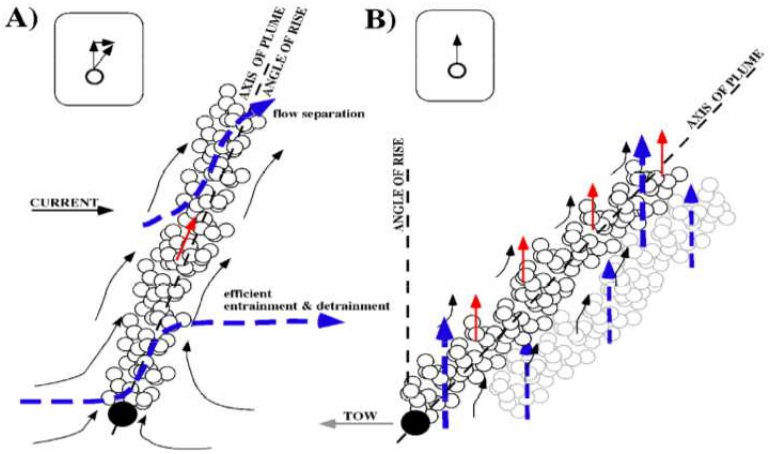


Fig. 6. Two dimensional schematic of a bubble plume for A) a fixed bubble source in a uniform horizontal current and B) towed bubble source through quiescent water. Inset shows details of individual bubble motions. Red and black arrows pertain to bubbles and entrained water, respectively. Grayed bubbles represent plume several seconds earlier, and remnant, persistent fluid motions.

For a stationary (i.e., fixed) source bubble plume in a uniform horizontal current, each bubble rises and is advected by the horizontal currents. As a result, the fluid motions and bubble plume motions are aligned along the plume axis. This allows the bubbles to accelerate the fluid throughout the entire water column. In contrast, for quiescent water (Fig. 6B). Bubbles rise vertically. Thus, for a towed bubble source, the apparent plume angle is vertical as are the fluid motions. However, they are not aligned with the angle of the plume. As a result, a parcel of water experiences vertical advection as a short pulse from the passing bubble sheet, rather than a sustained force. Thus, a towed bubble plume is more analogous to a bubble plume pulse in a horizontal current. Locally the two are identical; however, the boundary conditions are different. For a stationary bubble plume in a horizontal current (Fig 6A), the bubble plume is surrounded by water with no vertical motion. In contrast, in a towed plume the "local" bubble pulse is bounded on the down-tow side by persistent upwelling flows driven by the pulse that already passed. The primary bubble processes underlying the bubble plume trawl are bubble flotation and plume upwelling.

### 3.4 Towed submerged bubble rafts

Two highly distinct approaches were used to generate bubble plumes during the two field test series in 2008 and 2009 (Grimaldo et al, 2010). One, a bubble raft with tow parallel sparging elements, used a flushed sparger that tended to produce very small bubbles (which a video camera mounted on the raft imaged as milky in appearance) (Fig. 7A-B). The second, a bubble raft with tow transverse sparging elements, used a porous rubber hose that produced larger bubbles (~1-2 mm diameter) (Fig. 7C-D). The tow parallel bubble raft sought to maximize attachment flotation, while the tow transverse bubble raft was designed for using upwelling flotation.

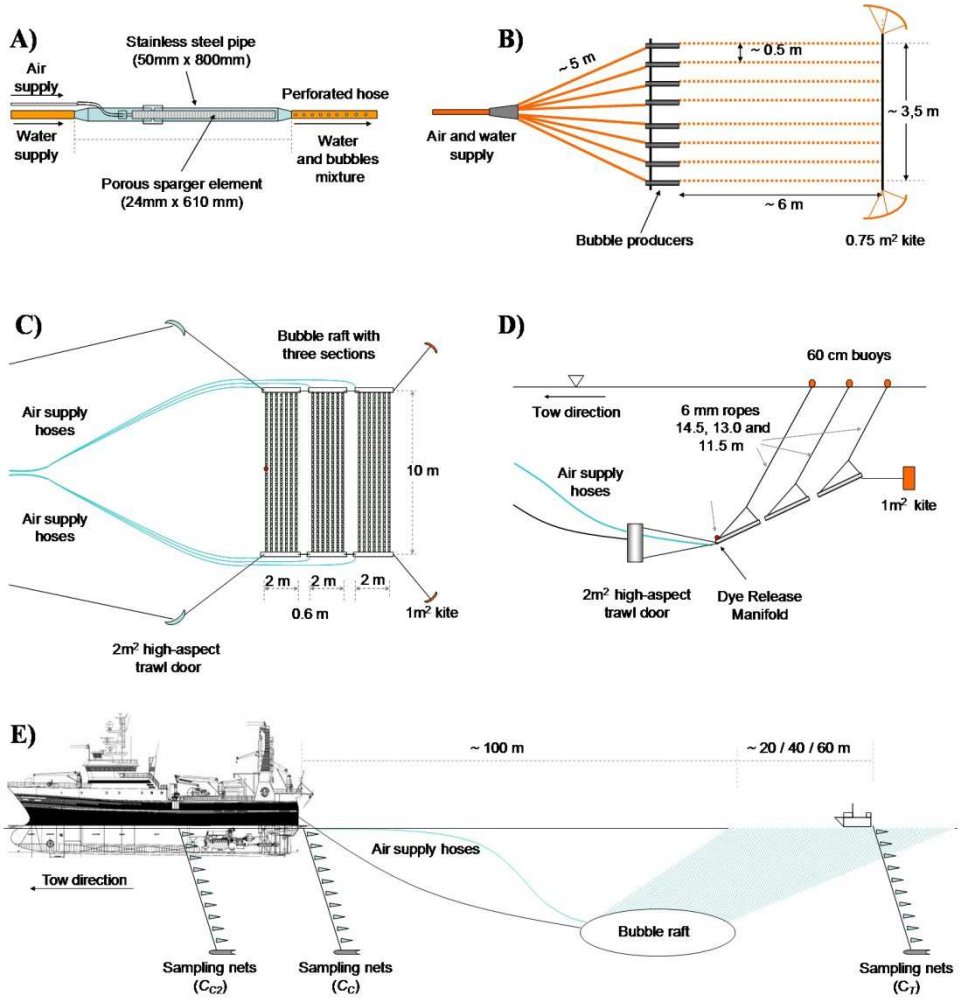


Fig. 7. Schematics for the bubble rafts: (A) Single bubble sparger element. (B) Top view of the raft with tow-parallel sparging elements. (C) Top view of the raft with tow-transverse sparging elements comprised of 3 sub-raft elements and (D) side view. (E) Bubble raft and plankton net deployment (Taken from Grimaldo et al., 2010).

Size distributions were not measured in the field (i.e., at depth, and under tow, and pressure) and significant deviations from laboratory bubbles are likely. With regards to bubble processes, the smaller flushed sparger bubbles are less efficient at creating upwelling flows (Patro *et al*., 2002), but more efficient at attachment (own data, unpublished) than the larger bubbles from the porous rubber hose. Significantly, bubbles from the flushed sparger from 25-m depth did not always reach the surface, strongly suggesting that the bubbles produced were dissolving during rise. Bubble dissolution reduces the buoyancy flux, decreasing the plume's ability to transport fluid against stratification and maintain coherency against current and wave disruption.

Plume upwelling velocities, $V_{up}$, were measured for the raft with tow-parallel sparging elements in the experiments of 2008 by injecting dye and measuring the transit time, $t$, for the dye to reach the sea surface. Values of $t$ were determined with a stopwatch based on the first arrival time at the sea surface, when the boil exhibited green colour (Fig. 8C); and generally showed a high degree of repeatability. Measurements were made for a range of airflows, $Q$ (2100 to 7200 L min$^{-1}$ at STP), and release depths, $z_0$ (2.5, 5.0, and 7.5 m). Each combination had between 3 and 20 repetitions, depending on variability (more repetitions for higher variability data sets). For the raft with tow transverse sparging elements, the upwelling flow was measured for $z_0$ = 15 m and $Q$ = 8432 L min$^{-1}$ (STP). However, dye surfacing was difficult to observe and $V_{up}$ was measured only for this combination. $V_{up}$ values were highly variable, but were mainly dependent on the air flow ($Q$). $V_{up}$ ranged between ~10 and 25 cm s$^{-1}$ and could be described by a power law fit, $V_{up} = Q^b$, where $b$ varied between 0.246 and 0.323, depending on release depth ($z_o$). $V_{up}$ for $z_o$>7.5 m were unsuccessful at advecting dye to the sea surface. For the raft with tow-transverse sparging elements, $V_{up}$ was measured (in 2009) for the maximum airflow rate ($Q$=8432 L min$^{-1}$) only and was 17.3±2.4 cm s $^{-1}$ for $z_o$=15 m.

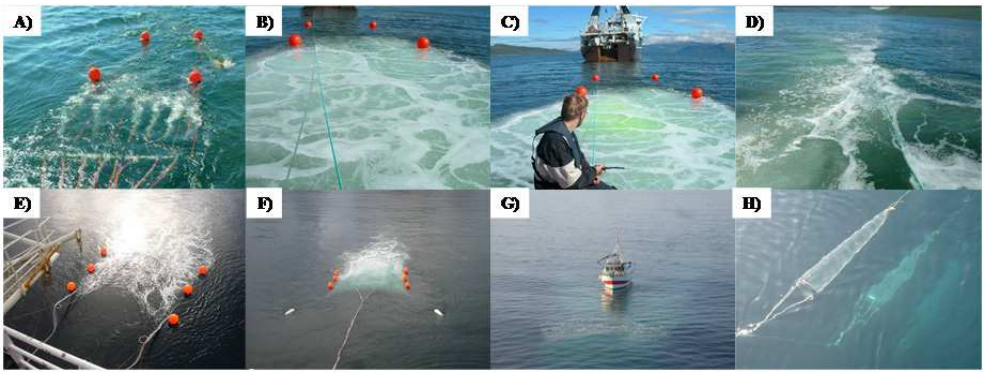


Fig. 8. Photos of the raft with tow-parallel sparging elements: A) During deployment 20 June 2008, B) Surface expression of the bubble plume for 4800 L min$^{-1}$ air from 5-m depth. C) Dye arriving at sea surface. Buoys are 60-cm diameter. *R/V Jan Mayen* stern is 120 m distant. D) Surface bubble plume for 25 m deployment. Photos of raft with tow-transverse sparging elements: E) During deployment on 29 April 2009. F) The trawl doors spreading the bubble raft laterally. G) *R/V Hyas* in position in bubble plume for sampling. H) Tow sampling nets, note high visibility.

The towed submerged bubble rafts were highly successful at elevating *Calanus* concentrations in a thin surface layer. Surface enhancements, $\varepsilon$, as high as 1416% were observed in full scale experiments off the coast of Troms, northern Norway, in 2009. Although greater $\varepsilon$ in surface layers were observed in 2008 in the presence of stratification, enhancement relative to the maximum in the water column, $C_C$, was far greater for the unstratified conditions of 2009 than 2008. In 2009, a *Calanus* trawl located at 20 m behind the bubble plume and fishing the upper meter would have in average increased the catch by 980%.These enhancements are dramatically larger than from hull mixing, which could not elevate *Calanus* concentrations greater than elsewhere in the water column (Fig 9).

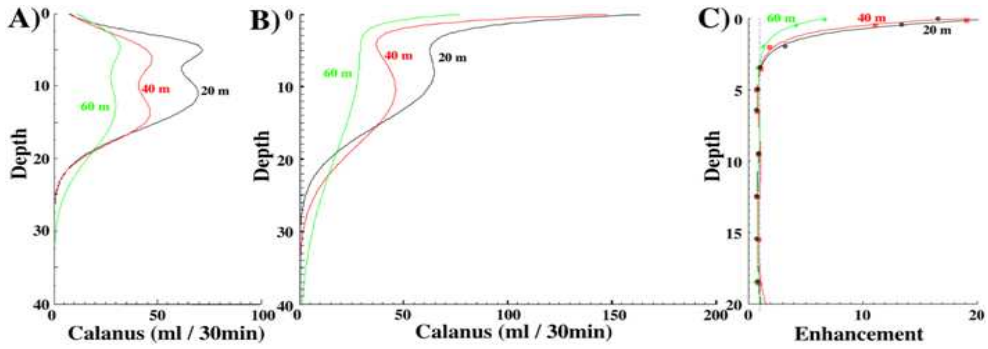


Fig. 9. Curve fits to *Calanus* sampling data for 29-30 April 2009, at 20, 40, and 60 m behind first bubble surfacing location. Data is not shown for clarity. A) Control plankton nets ($C_C$) B) Test plankton nets ($C_T$) and C) Enhancement ($\varepsilon$) based on curve fits (line) and data (symbols).

### 3.5 A continuous injection bubble pulse

The raft with tow-transverse sparging elements produced a truly novel bubble plume, continuously injecting bubbles into the same volume. Where a bubble pulse is produced from a stationary area plume and $Q$ increases as the bubble plume rises due to decreasing hydrostatic pressure, the increase in buoyancy flux is non-linear, and except for near the sea surface, small. For example, for a 20-m plume with $V_{up}$=20 cm s$^{-1}$, $Q$ doubles after bubbles have risen for 50 s. In comparison, the towed bubble raft's $Q$ for the first meter doubles after 1 second during which the plume has only risen ~0.5 m, with additional increases in $Q$ from hydrostatic expansion. On the other hand, because the bubble plume locally is a pulse, fluid acceleration is continuous. The upwelling flow generated was far less for the raft with tow-parallel sparging elements than for the raft with tow-transverse sparging elements due largely to the pulse-like nature of the bubble plume. Currently, bubble pulse behaviour, particularly for an area plume, remains completely uncharacterized, while this is the first reported continuous-injection bubble pulse.

### 3.6 Synergistic upwelling and flotation

Although the focus of the raft with tow-parallel sparging elements was attachment flotation and that of the raft with tow-transverse sparging elements was upwelling flotation, both processes occurred for both rafts. Moreover, the two processes are synergistic, *Calanus* with attached bubbles likely have greater difficulty escaping from the bubble plume, including when trapped in a turbulence vortex, and the added buoyancy increases their upwards velocity. Further, for *Calanus* to escape the bubble trawl, they need to jump away from the bubbles, which likely is less efficient for individuals with attached bubbles. One interesting and potentially important feature of vortex trapping is that it places zooplankton and bubbles in close proximity with numerous opportunities for bubble-zooplankton interaction and aggregation formation. Thus, significant *Calanus* could have some bubble attachment, aiding the upwelling process. Also, upwelled zooplankton likely becomes trapped in vortices, and the upwelling flow prevents downward escape. Lateral escape for zooplankton, even at the plume edge, likely is inefficient because of the inflow and the jump response is random when

confronted by bubbles (own data, unpublished). Further, some fraction of *Calanus* that do escape may be re-entrained in the upwelling flow in the bubble plume.

Because the enhancement, $\varepsilon$, for depths shallower than ~4 m was significantly above 1, but there was no significant reduction ($\varepsilon$<1) for deeper depths, increased *Calanus* in the water column must have been primarily from lateral bubble plume entrainment of *Calanus*. Some of the lateral entrainment could have arisen from deeper water ($z$>4 m), compensating in part for the reduction in $C_T(z)$ due to vertical advection (upwelling) of a *Calanus* profile $C_C(z)$ that decreased with depth below 10-12 m. However, enhancements of 560–980% relative to the water column maximum are difficult to explain by deeper entrainment and upwelling as they would almost certainly have caused a significant deviation from $\varepsilon$=1 for $z$>4 m. Given the absence of *Calanus* in the surface layer ($C_C$), lateral enhancement likely included an upwards component. Also, momentum plume upwelling, which surrounds the bubble plume, could have played a role through lateral *Calanus* entrainment.

### 3.7 Bubble trawl bycatch reduction

The upwelling flow and the vortices appeared to be effective at trapping other copepod-sized species, although healthy fingerlings were not caught, suggesting that they were not upwelled of lifted by bubble attachment. The towed bubble plume reduced by 65% of all types of bycatch organisms, which were in the path of the bubble plume. The greatest reduction was for crabs (in different larvae stages) and fish eggs, which initially were concentrated in a shallow layer (<3 m) and likely were floated towards the sea surface by the bubble plume. At the surface, the effect of the outwelling flow apparently removed them laterally, making them unavailable for the sampling nets. Because sampling was not performed at the bubble plume edges, the fate of these bycatch organisms is unclear. The bubble plume's effect upon fish larvae and especially upon small fish seems different from that for crab larvae and fish eggs. Accordingly, while the bubble attachment processes may have enhanced the flotation of crabs and fish eggs (presumably because of hair and stickiness of fish eggs); bubble attachment to fish larvae and fingerlings seems highly improbable. Also, visual evidence of small fish swimming inside the bubble plume suggests that fish larvae and fingerlings may have actively avoided the bubble plume. The largest (~3-4 mm diameter) bubbles surfaced first and apparently were highly effective for jellyfish flotation. This not only represents a great advantage for bubble-enhanced *Calanus* harvesting, but also for conventional fine-meshed trawls for *Calanus* and other fisheries. For example, jellyfish flotation could divert jellyfish from the trawl path, avoiding associated problems with net clogging, catch damage, sorting, etc. Jellyfish flotation appears distinct from *Calanus* flotation, in that due to the morphology of the jellyfish, bubbles readily are trapped in their body, leading to more effective buoyant rise. For example, jellyfish were very common in 2008 and were observed floating at the sea surface with entrapped bubbles. Although the bubble trawls were not designed to effectively divert jellyfish through flotation; such diverters could be very useful for improving the *Calanus* fishery.

## 4. Conclusion

The area bubble plume-enhanced *Calanus* harvesting technology is a unique and novel design that improved copepod catch rates, reduced bycatch, and significantly decreased energy consumption during towing by allowing for a smaller collector. Results showed very

strong *Calanus* enhancement relative to elsewhere in the water column in a thin surface layer during tests in the absence of stratification. Stratification was a dominant factor affecting bubble trawl performance; however, data were insufficient to characterize stratification's effect on bubble plume fluid motions beyond fluid-ambient density difference. Investigation of the bubble generation approach suggested small bubbles are problematic, particularly for deeper tow depths where dissolution becomes significant, compared to larger bubbles. Large bubble generation was effective by pressurizing a porous rubber hose – the pressure difference across the hose walls prevented hydrostatic pressure changes (swell) from causing emission variability along the sparger elements, in contrast to a drilled rubber hose. The current bubble trawl design, while appropriate for these field tests, lacked robustness for commercial application. Although highly promising, results highlighted significant areas of critical need for further study: increased sampling resolution, validation of the vortex *Calanus* trapping hypothesis, and characterization of the role of stratification in bubble plume processes related to bubble trawl performance.

## 5. Acknowledgment

This chapter is based on results that have been obtained through diverse research projects mainly funded by the Research Council of Norway, and the Norwegian industry. We gratefully acknowledge the inspiring discussions with many researchers involved in these projects. Particular thanks goes to Birger Enerhaug (SINTEF), Thomas McClimas (SINTEF), Ira Leifer (University of California), Snorre Angell (Calanus AS), Roger B. Larsen, Ivan Tatone and Trond Larsen (University of Tromsø), and the crews of R/V Hyas and R/V Jan Mayen.

## 6. References

Aksnes D.L. and Blindheim J. (1996). Circulation patterns in the North Atlantic and possible impact on population dynamics of *Calanus finmarchicus*. *Ophelia,* Vol. 44, pp. 7–28.

Aseda, T. and Imberger, J.T. (1993). Structure of bubble plumes in linearly stratified environments. *Journal of Fluid Mechanics*, Vol. 249, pp. 35-57.

Brundrett, E. (1993). Prediction of pressure drop for incompressible flow through screens. *Journal of Fluids Engineering,* Vol. 115, pp. 239–242.

Cumberbatch, E. (1982). Two-dimensional flow past a mesh. *Quarterly Journal of Mechanics and Applied Mathematics*, Vol. 35, No. 3, pp. 335-344.

Dahle, T., Kaartvedt, S. (2000). Diel patterns in stage-specific vertical migration of *Calanus finmarchicus* in habitats with midnight sun. *ICES Journal of Marine Science,* 57, 1800-1818.

Falkenhaug, T., Timonin, T., Tande, K. (1997). Abundance and distribution of numerical important species of zooplankton in summer and winter periods of 1990 and 1991 in North Norwegian fjords. *Journal of Plankton Research,* Vol. 19, No. 4, pp. 449-468.

Fanneløp, T. K., Webber, D. M. (2003). On buoyant plumes rising from area sources in a calm environment, *Journal of Fluid Mechanics,* Vol. 497, pp. 319-334.

Gibbings, J.C. (1973). The pyramid gauze diffuser. Ingenieur-Archiv Vol. 42, pp. 225–233.

Gjøsund, S.H. (2006). Flow through nets and trawls of high solidity. SINTEF Fisheries and Aquaculture report no. SFH80 A063012, ISBN 82-14-03872-3, Trondheim, January 2006.

Gjøsund, S.H., Enerhaug, B. (2010). Flow through nets and trawls of low porosity. *Ocean Engineering*, Vol. 37, No. 4, pp. 345-354.

Grimaldo, E., Leifer, I., Gjøsund, S.H., Larsen, R.B., Jeuthe, H., Basedow, S. (2010). Field demostration of a novel towed, area bubble-plume zooplankton (*Calanus sp.*) harvester. *Fisheries Rersearch*, Vol. 107, pp. 147-158.

Johnson, B. D., Cooke, R. C. (1980). Organic Particle and Aggregate Formation Resulting from the Dissolution of Bubbles in Seawater. *Limnology and Oceanography,* Vol. 5, No. 4, pp. 653-661.

Harris, R.P., Wiebe, P.H., Lenz, J., Skjoldal, H.R., and Huntley, M. (Eds.), (2000). *ICES Zooplankton Methodology Manual*. Academic Press.

Kattner, G. and Krause, M. (1987). Changes in lipids during the development of *Calanus finmarchicus* s.l. from Copepodid I to adult. *Marin Biology*, Vol. 96, pp. 511–518.

Lalli, C. M., Parsons, T. R. (1997). *Biological Oceanography*. ISBN 0750633840, The Open University.

Larsen, T. (2009). Slepemotstand, effektivitet og fangstsammensetning i fiske med trål tilpasset dyreplankton - Forsøk med trål i småskala. MSc thesis, The Norwegian College of Fishery Science, University of Tromsø, February 2009.

Leifer, I., Boles, J. (2005). Measurement of marine hydrocarbon seep flow through fractured rock and unconsolidated sediment. *Marine and Petroleum Geology*, Vol. 22, No. 4, pp. 551-568.

Leifer, I., Jeuthe, H., Gjøsund, S.H., Johansen, V. (2009). Engineered and natural marine seep, bubble driven buoyancy flows. *Journal of Physical Oceanography*, Vol. 39, No. 12, pp. 3071-3090.

Leifer, I., Clark, J.F., Chen, R.F. (2000). Modifications to the local environment by natural marine hydrocarbon seeps. *Geophysical Research Letters*, Vol. 27, pp. 3711-3714.

Leifer, I., Luyendyk, B., Boles, J., Clark, J.F. (2006). Natural marine seepage blowout: Contribution to atmospheric methane. *Global Biogeochemical Cycles*, Vol. 20, GB3008, doi: 10.1029/2005GB002668, pp. 1-9,

Leifer, I., Patro, R. K. (2002). The bubble mechanism for methane transport from the shallow sea bed to the surface: A review and sensitivity study. *Continental Shelf Research*, Vol. 22, No. 16, pp. 2409-2428.

Leifer, I., Judd, A. (2002). Oceanic methane layers: A bubble deposition mechanism from marinehydrocarbon seepage. *Terra Nova,* Vol. 16, pp. 471-485.

Lemckert, C.J., Imberger, J. (1993). Energetic bubble plumes in arbitrary stratification. *Journal of Hydraulic Engineering,* Vol. 119, pp. 680-703.

List, E.J. (1982). Turbulent jets and plumes. *Annual Review of Fluid Mechanics,* Vol. 14, pp. 189–212.

Løland, G. (1991). Current forces on and flow through fish farms. Doctoral thesis, Dept. of Marine Hydrodynamics, The Norwegian Institute of Technology.

Mao, L., Yoon, R.-H. (1997). Prediction flotation rates using a rate equation derived from first principles. *International Journal Mineral Processing*, Vol. 51, pp. 171-181.

Mari, X. (1999). Carbon content and C:N ratio of transparent exopolymeric particles (TEP) produced by bubble exudates of diatoms. *Marine Ecology Progress Series,* Vol. 183, pp. 59-71.

McDougall, T.J. (1978). Bubble plumes in stratified environments. *Journal of Fluid Mechanics,* Vol. 85, pp. 655-672.

McQueen, D.J., Yan, N.D. (1993). Metering filtration efficiency of freshwater zooplankton hausl: reminders from the past. *Journal of Plankton Research*, Vol. 15, Vol. 1, pp. 57-65.

Milgram, J.H. (1983). Mean flow in round bubble plumes. *Journal of Fluid Mechanics,* Vol. 133, pp. 345-376.

Mizukawaa, K., Takada, H., Takeuchi, I., Ikemoto, T., Omori, K., Tsuchiya, K. (2009). Bioconcentration and biomagnification of polybrominated diphenyl ethers (PBDEs) through lower-trophic-level coastal marine food web. *Marine Pollution Bulletin,* Vol. *58, No.* 8, pp. 1217-1224

Nicol, S., Endo, Y. (1999). Krill fisheries: Development, management and ecosystem implications. *Aquatic Living Resources,* Vol. 12, No. 2, pp. 105-120.

Patro, R.K., Leifer, I., Bowyer, P. (2002). Better bubble process modelling: Improved bubble hydrodynamics parameterization. In: *Gas Transfer at Water Surfaces*, M.Donelan, (Ed.). American Geophysical Union, Washington, pp. 315-320.

Persechini, M.A.M., Jota, F.G., Peres, A.E.C. (2000). Dynamic model of a flotation column. *Minerals Engineering*, Vol. 13, pp. 1465-1481.

Reynolds, A.J. (1969). Flow deflection by gauze screens. Journal of Mechanical Enginering Science, Vol. 11, pp. 290-294.

Schadlow, G. (1992). Bubble plume dynamics in a stratified medium and the implications for water quality amelioration in lakes. *Water Resources Research*, Vol. 28, No. 2, 313-321.

Schubauer, G.B., Spangenberg, W.G., and Klebanoff, P.S. (1950). Aerodynamic characteristics of damping screens. NACA Technical note no. 2001.

Singleton, V. L., Gantzer, P., Little, J.C. (2007). Linear bubble plume model for hypolimnetic oxygenation: Full-scale validation and sensitivity analysis. *Water Resources Research*, Vol. 43. Wo2405, Doi:10.1029/2005WR004836, pp. 1-12.

Skjoldal, H.R., Dalpadado, P., Dommasnes, A. (2004). Food webs and trophic interactions. *In: The Norwegian Sea ecosystem, Skjoldal HR (*Ed.*)*. Tapir Academic, Trondheim, Norway, pp. 447—506

Skjoldal, H.R. (2005). *The Norwegian Sea Ecosystem*, Tapir Academic Press.

Solomon, E.A., Kastner, M., MacDonald, I.R., Leifer, I. (2009). Considerable methane fluxes to the atmosphere from hydrocarbon seeps in the Gulf of Mexico. *Nature Geoscience*, Vol. 2, pp. 561-565.

Sournia, A. (Ed.), (1978). *Phytoplankton manual*. UNESCO, Paris, 1978.

Tande, K. S., Miller, C.B. (2000). Population dynamics of *Calanus* in the North Atlantic: Results from the trans-Atlantic study of *Calanus finmarchicus*. *ICES Journal of Marine Science,* Vol. 57, No. 6, pp. 1527-1527.

Taylor, G.I. and Batchelor, G.K. (1949). The effect of wire gauzes on small disturbances in a uniform stream. *Quarterly Journal of Mechanics and Applied Mathematics*, Vol. 2, pp. 1-29.

Topham, D.R. (1975). Hydrodynamics of an oil well blowout. Beaufort Sea Technical Report, Institute of Ocean Science, Sidney BC, No 33.

Tranter, D.J., and Heron, A.C. (1967). Experiments on filtration in plankton nets. *Australian Journal of Marine Freshwater Research*, Vol. 16, pp. 281-291.

Unstad, K., Tande, K. (1991). Depth distribution of *Calanus finmarchicus* and *C. glacialis* in relation to environmental conditions in the Barents Sea. *Polar Research,* Vol. 10, No. 2, pp. 409-420.

Wiborg, K.F., Hansen, K. (1974). Fiske og utnyttelse av raudåte (*Calanus finmarchicus*). Fisken og Havet, Serie B, Vol. 10, pp. 1-25, Institute of Marine Research, Bergen.

Wu, J. (1995). Mechanisms of animal cell damage associated with gas bubbles and cell protection by medium additives. *Journal of Biotechnology*, Vol. 43, pp. 81-94.

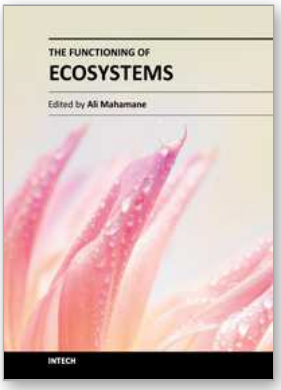


**The Functioning of Ecosystems**

Edited by Prof. Mahamane Ali

ISBN 978-953-51-0573-2
Hard cover, 332 pages
**Publisher** InTech
**Published online** 27, April, 2012
**Published in print edition** April, 2012

The ecosystems present a great diversity worldwide and use various functionalities according to ecologic regions. In this new context of variability and climatic changes, these ecosystems undergo notable modifications amplified by domestic uses of which it was subjected to. Indeed the ecosystems render diverse services to humanity from their composition and structure but the tolerable levels are unknown. The preservation of these ecosystemic services needs a clear understanding of their complexity. The role of the research is not only to characterise the ecosystems but also to clearly define the tolerable usage levels. Their characterisation proves to be important not only for the local populations that use it but also for the conservation of biodiversity. Hence, the measurement, management and protection of ecosystems need innovative and diverse methods. For all these reasons, the aim of this book is to bring out a general view on the biogeochemical cycles, the ecological imprints, the mathematical models and theories applicable to many situations.



**InTech Europe**
University Campus STeP Ri
Slavka Krautzeka 83/A
51000 Rijeka, Croatia
Phone: +385 (51) 770 447
Fax: +385 (51) 686 166
www.intechopen.com

**InTech China**
Unit 405, Office Block, Hotel Equatorial Shanghai
No.65, Yan An Road (West), Shanghai, 200040, China
中国上海市延安西路65号上海国际贵都大饭店办公楼405单元
Phone: +86-21-62489820
Fax: +86-21-62489821